PERGAMON

International Journal of Heat and Mass Transfer 43 (2000) 3673–3686

International Journal of HEAT and MASS TRANSFER

www.elsevier.com/locate/ijhmt

Combined forced and free flow of a power-law fluid in a vertical annular duct

A. Barletta

Dipartimento di Ingegneria Energetica, Nucleare e del Controllo Ambientale (DIENCA), Università di Bologna, Viale Risorgimento 2, I-40136 Bologna, Italy

Received 8 October 1999

Abstract

An investigation of mixed convection and flow reversal in a vertical annular duct is presented with reference to laminar and fully-developed flow of a power-law fluid. The boundary surfaces are supposed to be isothermal, with unequal temperatures. The momentum balance and the energy balance equations as well as the viscous stress constitutive equation are solved analytically in order to obtain the velocity field, the viscous stress field and the temperature field. First, two special cases are analyzed: mixed convection of a Newtonian fluid; forced convection of a power-law fluid. Then, in the general case, the evaluation of the friction factors is employed to determine the conditions for the occurrence of flow reversal, for fixed values of the power-law index and of the ratio between the duct inner and outer radii.

Keywords: Mixed convection; Non-Newtonian fluids; Laminar flow; Analytical methods

1. Introduction

Many industrial applications involve paints, glues, inks, soap as well as suspensions such as coal-water slurries. As is well known, these fluids display a behavior definitely different from that of Newtonian fluids. Several papers dealing with the heat transfer of non-Newtonian fluids in ducts have appeared in the literature. Reviews of the most important results obtained for internal flow convection of non-Newtonian fluids are available in the literature [1–5]. Recently, some novel investigations on laminar flow forced convection of non-Newtonian fluids in ducts have been presented [6–15]. Gao and Hartnett [6] are concerned with the fully developed forced convection of power-law fluids in rectangular ducts. Capobianchi and Irvine [7] provide a numerical evaluation of the velocity and temperature profiles for the fully developed forced convection of a modified power-law fluid in an annular duct. Prusa and Manglik [8] describe a finite difference solution of the classical Nusselt-Graetz problem in a circular duct, with reference to a power-law fluid. The finite element method is employed by Etemad and Mujumdar [9] to obtain a solution for the simultaneously-developing laminar forced convection in a semicircular duct for a power-law fluid with a temperature-dependent consistency index. In Ref. [10], an analysis of the boundary conditions which ensure the existence of a thermally developed region in the case of laminar forced convection with viscous dissipation is performed, with reference to power-law

E-mail address: antonio.barletta@mail.ing.unibo.it (A. Barletta).

0017-9310/00/$ - see front matter
PII: S0017-9310(00)00006-5

Nomenclature

a, b, w, z	dummy complex variables
$B_z(a,b)$	incomplete Euler beta function
$C(m,\gamma,\Lambda)$	root of Eq. (22)
D	hydraulic diameter, $D = 2R_2(1-\gamma)$ (m)
f_1, f_2	inner and outer friction factors defined by Eq. (17)
${}_2F_1(a, b; w; z)$	hypergeometric function
g	modulus of the gravitational acceleration (m s^{-2})
Gr	Grashof number defined by Eq. (9)
m	inverse of the power-law index
p	fluid pressure (Pa)
P	difference between the pressure and the hydrostatic pressure, $P = p + \rho_0 gX$ (Pa)
R	radial coordinate (m)
r	dimensionless radial coordinate defined by Eq. (9)
R_1, R_2	inner and outer radii of the duct (m)
Re	Reynolds number defined by Eq. (9)
T	temperature (K)
T_0	mean temperature in a duct section (K)
T_1, T_2	inner and outer wall temperatures (K)
U	axial component of velocity (m s^{-1})
U_0	reference velocity defined by Eq. (8) (m s^{-1})
$\bar{U}$	mean velocity in a duct section (m s^{-1})
u	dimensionless velocity defined by Eq. (9)
$u_{\max}$	maximum dimensionless velocity in a duct section
$\bar{u}$	mean dimensionless velocity in a duct section
V	radial component of velocity (m s^{-1})
X	axial coordinate (m)
β	thermal expansion coefficient (K^{-1})
γ	dimensionless parameter defined by Eq. (9)
$\Gamma(z)$	Euler gamma function
η	consistency factor (Pa s$^{1/m}$)
θ	dimensionless temperature defined by Eq. (9)
Λ	dimensionless parameter defined by Eq. (9)
Λ_r, Λ_r'	threshold values of Λ for the onset of flow reversal
ρ	mass density (kg m^{-3})
ρ_0	mass density at temperature T_0 (kg m^{-3})
σ	dimensionless shear stress defined by Eq. (9)
τ, τ_{RX}, τ_{XR}	shear stresses (Pa)
ω	dimensionless parameter defined by Eq. (9)

fluids in circular ducts. Min et al. [11,12] provide a wide analysis of forced convection in a circular duct for a Bingham plastic. In particular, in Refs. [11,12], the fully developed and the thermally developing regimes are studied by employing analytical methods, namely Frobenius method and separation of variables, while the hydrodynamically developing regime is analyzed by a numerical technique based on the Crank–Nicolson scheme. Khellaf and Lauriat [13] evaluate analytically both the bulk temperature and the local Nusselt number for the thermally developing forced convection either in a parallel-plate channel or in a circular duct, with reference to a power-law fluid and to a boundary condition of uniform wall temperature. By employing a finite integral transform technique, Lawal and Kalyon [14] investigate forced convection flow with viscous dissipation for a Herschel–Bulkley fluid flowing between two parallel plates in relative motion. Olek [15] develops a general analytical method to obtain the temperature field in the thermal entrance region of a circular or parallel-plate duct with convective boundary conditions. Olek's solution holds for laminar forced convection even if axial heat conduction in the fluid cannot be neglected and can be employed for an arbitrary fully developed velocity profile, i.e. for an arbitrary Newtonian or non-Newtonian fluid.

The effect of buoyancy forces in non-Newtonian fluid flow has been investigated by Jones and Ingham [16] and by Ingham and Jones [17]. In Refs. [16,17], a study of the mixed convection flow in the entrance region of a vertical parallel-plate channel is performed. Reference is made either to uniform wall temperatures [16] or to linearly varying wall temperatures [17]. In both cases, solutions for the streamfunction, vorticity and temperature fields are determined by employing a finite difference method.

Recently, an analytical solution for the velocity profiles of a power-law fluid in the fully developed region of a parallel-plate vertical channel has been obtained in the case of mixed convection with asymmetric and

uniform wall temperatures [18]. Moreover, in the same paper, the conditions for the occurrence of flow reversal are determined both for upward flow and for downward flow. Indeed, an extension of the analysis performed in Ref. [18], to investigate mixed convection flows in vertical annular ducts appears as interesting.

The subject of mixed convection in vertical annular ducts has been studied by several authors [19–22]. The papers by Sherwin [19], Rokerya and Iqbal [20], Maitra and Sabba Raju [21] refer to Newtonian fluids and to a uniform wall heat flux prescribed either on the inner wall [19–21] or on the outer wall [20]. On the other hand, in the paper by Kou and Huang [22], a non-Darcian flow model is employed to investigate mixed convection in a vertical annular duct filled with a porous medium.

The aim of the present paper is to extend the mathematical model considered in Ref. [18], as well as the analytical method employed to solve the governing equations, in order to analyze the combined forced and free flow of a power-law fluid in a vertical annular duct. The analysis will be performed under the hypothesis of laminar and fully developed flow. Moreover, the duct walls will be supposed to be isothermal, with different temperatures. In the following sections, it will be pointed out that, both for Newtonian and non-Newtonian fluids, the value of the pressure gradient which is required to produce a given mass flow rate is influenced by the buoyancy effect. On the other hand, in Ref. [18] it is shown that, in the case of a vertical parallel-plate channel, this feature occurs only for non-Newtonian fluids, while Newtonian fluids display the same relation between pressure gradient and mass flow rate both for forced convection and for mixed convection.

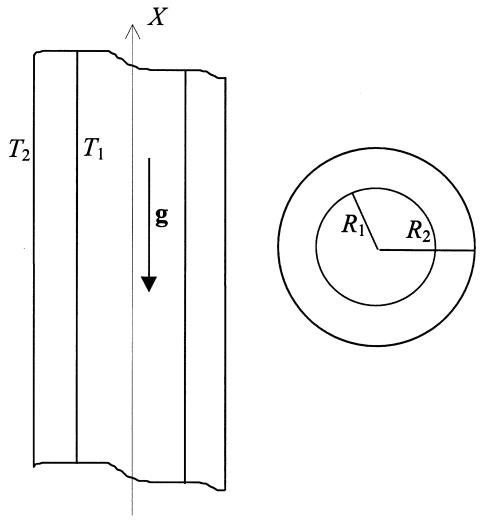

Fig. 1. Drawing of the system.

2. Formulation of the problem

In this section, the heat transfer problem is described and the set of governing equations is expressed in a dimensionless form.

Let us consider the vertical annular duct shown in Fig. 1. The thermal boundary conditions are such that the internal wall is isothermal with a temperature T_1, while the external wall is isothermal with a temperature $T_2 \neq T_1$. Viscous dissipation is neglected and the flow is assumed to be steady, laminar and fully developed. The Boussinesq approximation and the mass balance equation imply that the velocity field is solenoidal, while the condition of fully developed flow implies that $\partial U/\partial X = 0$. Therefore, one can conclude that U depends only on R and that V is zero. Moreover, it can be inferred that the only nonvanishing component of the viscous stress tensor is $\tau = \tau_{RX} = \tau_{XR}$. The latter is assumed to be expressed by the Ostwald–De Waele constitutive equation, namely

$$\tau = \eta \left| \frac{\mathrm{d}U}{\mathrm{d}R} \right|^{(1-m)/m} \frac{\mathrm{d}U}{\mathrm{d}R}. \tag{1}$$

Eq. (1) implies that the case $m < 1$ corresponds to dilatant fluid behavior, while the case $m > 1$ corresponds to pseudoplastic fluid behavior.

The buoyancy effect is accounted for by employing the equation of state

$$\rho = \rho_0 \left[1 - \beta (T - T_0) \right], \tag{2}$$

where ρ_0 and β are assumed to be constant and T_0 is chosen as the mean temperature in a duct section, i.e.

$$T_0 = \frac{2}{R_2^2 - R_1^2} \int_{R_1}^{R_2} TR \, \mathrm{d}R. \tag{3}$$

The choice of the reference temperature expressed by Eq. (3) ensures the best conditions for the validity of the Boussinesq approximation [23]. Let us assume that the thermal conductivity of the fluid and the consistency factor η are independent of temperature. Since η is a constant, Eq. (1) implies that τ depends only on R. The momentum balance in the radial direction yields $\partial P/\partial R = 0$, while the momentum balance in the X-direction can be expressed as

$$g\beta\rho_0 (T - T_0) - \frac{\mathrm{d}P}{\mathrm{d}X} + \frac{1}{R} \frac{\mathrm{d}}{\mathrm{d}R} (R\tau) = 0. \tag{4}$$

If both sides of Eq. (4) are derived with respect to X, multiplied by R and then integrated with respect to R

in the interval $R_1 \le R \le R_2$, on account of Eq. (3), one can conclude that

$$\frac{d^2P}{dX^2} = 0, \qquad \frac{\partial T}{\partial X} = \frac{dT_0}{dX}. \tag{5}$$

Eq. (5) implies that dP/dX is a constant. Moreover, since $\partial T/\partial X$ is zero at the boundary walls and since Eq. (5) ensures that $\partial T/\partial X$ does not depend on R, one can conclude that T is independent of X. Therefore, the energy balance equation yields

$$\frac{d}{dR}\left(R\frac{dT}{dR}\right) = 0. \tag{6}$$

It can be easily proved that Eq. (1) can be rewritten as

$$\frac{dU}{dR} = \frac{\tau}{\eta}\left(\frac{|\tau|}{\eta}\right)^{m-1}. \tag{7}$$

If one chooses the reference velocity

$$U_0 = -\left(\frac{2}{\eta}\right)^m D^{m+1}\left|\frac{dP}{dX}\right|^{m-1}\frac{dP}{dX} \tag{8}$$

and defines the dimensionless quantities

$$\begin{gathered} Re = \frac{\rho_0 U_0 |U_0|^{(m-1)/m} D^{1/m}}{\eta}, \\ Gr = \frac{g\beta\rho_0^2 (T_2 - T_1)|U_0|^{2(m-1)/m} D^{(m+2)/m}}{\eta^2}, \\ \theta = \frac{T - T_0}{T_2 - T_1}, \\ r = \frac{R}{R_2}, \quad \gamma = \frac{R_1}{R_2}, \quad u = \frac{U}{U_0}, \quad \omega = \frac{T_0 - T_1}{T_2 - T_1}, \\ \sigma = \frac{2Re\tau}{\rho_0 U_0^2}, \quad \Lambda = \frac{Gr}{Re}, \end{gathered} \tag{9}$$

the governing Eqs. (4), (6) and (7) can be rewritten as

$$2(1-\gamma)\frac{d}{dr}(r\sigma) = -r(2\Lambda\theta + 1), \tag{10}$$

$$\frac{d}{dr}\left(r\frac{d\theta}{dr}\right) = 0, \tag{11}$$

$$\frac{du}{dr} = \frac{\sigma|\sigma|^{m-1}}{2^{m+1}(1-\gamma)}. \tag{12}$$

Eqs. (8) and (9) allow one to conclude that a *downward gradient flow* ($dP/dx < 0$) corresponds to $U_0 > 0$ and $Re > 0$, while an *upward gradient flow* ($dP/dx > 0$) corresponds to $U_0 < 0$, $Re < 0$. Then, for downward gradient flow, the parameter Λ is positive if $T_2 > T_1$, while it is negative if $T_2 < T_1$. Obviously, the opposite occurs in the case of upward gradient flow.

It is easily verified that the dimensionless fields are subjected to the boundary conditions

$$u(\gamma) = u(1) = 0, \quad \theta(\gamma) = -\omega, \quad \theta(1) = 1 - \omega. \tag{13}$$

Moreover, Eq. (2) implies that the dimensionless temperature θ must fulfil the constraints

$$\int_\gamma^1 \theta(r) r\, dr = 0. \tag{14}$$

If the ratio $\gamma = R_1/R_2$, the inverse of the power-law index m and the parameters

$$\Lambda = \frac{Gr}{Re} = \frac{g\beta D(T_2 - T_1)}{U_0^2} Re \tag{15}$$

are prescribed, the solution of Eqs. (10)–(14) allows one to obtain $u(r)$, $\theta(r)$, $\sigma(r)$ and the parameter ω. Let us define the dimensionless parameter $\bar{u}$ as

$$\bar{u} = \frac{\bar{U}}{U_0} = \frac{2}{1-\gamma^2}\int_\gamma^1 u(r) r\, dr. \tag{16}$$

Obviously, the ratio $\bar{u}$ between the mean velocity in a channel section $\bar{U}$ and the reference velocity U_0, may depend not only on m and γ, but also on Λ. In other words, the mass flow rate which occurs for a given value of the vertical pressure gradient may be influenced by the buoyancy effect.

The Fanning friction factors are defined as

$$f_1 = 2\frac{\tau(R_1)}{\rho_0 U_0^2} = \frac{\sigma(\gamma)}{Re}, \qquad f_2 = -2\frac{\tau(R_2)}{\rho_0 U_0^2} = -\frac{\sigma(1)}{Re}. \tag{17}$$

As a consequence of Eqs. (14) and (17), if one integrates both sides of Eq. (10) with respect to r in the interval $[\gamma, 1]$, one is led to a relation between the friction factors, namely

$$f_2 = \frac{1+\gamma}{4Re} - \gamma f_1. \tag{18}$$

Moreover, as a consequence of the no-slip conditions expressed in Eq. (13), an integration of both sides of Eq. (12) with respect to r in the interval $[\gamma, 1]$ yields a constraint on $\sigma(r)$, namely

$$\int_\gamma^1 \sigma(r)|\sigma(r)|^{m-1}\, dr = 0. \tag{19}$$

3. Evaluation of the velocity and stress fields

In this section, the dimensionless temperature, shear stress and velocity are determined by solving analytically Eqs. (10)–(14). Moreover, the special cases of mixed convection for Newtonian fluids and of forced convection are discussed.

One can easily integrate Eq. (11), so that Eqs. (14) and (16) allow one to obtain the dimensionless temperature distribution and the parameter ω,

$$\theta(r) = -\frac{\ln(r)}{\ln(\gamma)} - \frac{\gamma^2}{1-\gamma^2} - \frac{1}{2\ln(\gamma)},$$
$$\omega = \frac{1}{1-\gamma^2} + \frac{1}{2\ln(\gamma)}. \tag{20}$$

Then, Eqs. (10) and (20) allow one to obtain an expression of $\sigma(r)$, namely

$$\sigma(r) = \frac{2C(m,\gamma,\Lambda) - r^2}{4r(1-\gamma)} + \frac{\Lambda r}{2(1-\gamma)}\left(\frac{\ln(r)}{\ln(\gamma)} + \frac{\gamma^2}{1-\gamma^2}\right), \tag{21}$$

where $C(m, \gamma, \Lambda)$ is an integration constant. For given values of the parameters m, γ and Λ, the value of this constant can be determined by solving Eq. (19). More precisely, if one substitutes Eq. (21) in Eq. (19), then one obtains $C(m, \gamma, \Lambda)$ as the solution of the equation

$$\int_\gamma^1 \left[2C - r^2 + 2\Lambda r^2\left(\frac{\ln(r)}{\ln(\gamma)} + \frac{\gamma^2}{1-\gamma^2}\right)\right]\left|2C - r^2 + 2\Lambda r^2\left(\frac{\ln(r)}{\ln(\gamma)} + \frac{\gamma^2}{1-\gamma^2}\right)\right|^{m-1}\frac{dr}{r^m} = 0. \tag{22}$$

After having determined $\sigma(r)$ by employing Eqs. (21) and (22), the dimensionless velocity distribution is obtained as the solution of Eq. (12) which fulfils the no-slip conditions expressed by Eq. (13), namely

$$u(r) = \frac{1}{2^{m+1}(1-\gamma)}\int_\gamma^r \sigma(r')|\sigma(r')|^{m-1}\,dr'. \tag{23}$$

On account of Eqs. (17) and (21), the friction factors f_1 and f_2 can be expressed as

$$f_1 Re = \frac{2C(m,\gamma,\Lambda) - \gamma^2}{4\gamma(1-\gamma)} + \frac{\Lambda\gamma}{2(1-\gamma)^2(1+\gamma)},$$
$$f_2 Re = \frac{1 - 2C(m,\gamma,\Lambda)}{4(1-\gamma)} - \frac{\Lambda\gamma^2}{2(1-\gamma)^2(1+\gamma)}. \tag{24}$$

The solution of Eq. (22) can be easily determined for $m = 1$. In fact, for Newtonian fluids, one obtains

$$C(1,\gamma,\Lambda) = -\frac{1-\gamma^2}{4\ln(\gamma)}\left[1 + \frac{\Lambda}{\ln(\gamma)}\right]. \tag{25}$$

In the special case $m = 1$, Eqs. (21), (23) and (25) yield the dimensionless velocity profile

$$u(r) = \frac{(1-r^2)\ln(\gamma) - (1-\gamma^2)\ln(r)}{32(1-\gamma)^2\ln(\gamma)} - \Lambda\frac{(1-\gamma^2)\left[1-\gamma^2-2r^2\ln(\gamma)\right]\ln(r) - (1-r^2)\left[1-\gamma^2-2\gamma^2\ln(\gamma)\right]\ln(\gamma)}{32(1-\gamma)^3(1+\gamma)\left[\ln(\gamma)\right]^2}. \tag{26}$$

On account of Eqs. (16) and (26), the mean dimensionless velocity in a channel section is expressed as

$$\bar{u} = \frac{1-\gamma^2+(1+\gamma^2)\ln(\gamma)}{64(1-\gamma)^2\ln(\gamma)} + \Lambda\frac{2(1-\gamma^2)^2+(1-\gamma^4)\ln(\gamma) - 4\gamma^2\left[\ln(\gamma)\right]^2}{128(1-\gamma)^3(1+\gamma)\left[\ln(\gamma)\right]^2}. \tag{27}$$

Eq. (27) reveals that, for a Newtonian fluid, the parameter $\bar{u}$ depends on Λ. However, in the limit $\gamma\to 1$, this parameter becomes independent of Λ and is equal to 1/96. This result is in agreement with the analysis presented in Ref. [18] with reference to a parallel plate channel. Indeed, if $\gamma\to 1$, the flow in an annular duct becomes coincident with that in a parallel plate channel.

On account of Eqs. (24) and (25), in the special case $m = 1$, the friction factors can be expressed as

$$f_1 Re = -\frac{\gamma}{4(1-\gamma)} - \frac{1+\gamma}{8\gamma\ln(\gamma)} + \Lambda\left[\frac{\gamma}{2(1-\gamma)^2(1+\gamma)} - \frac{1+\gamma}{8\gamma\ln(\gamma)^2}\right],$$

$$f_2 Re = \frac{1}{4(1-\gamma)} + \frac{1+\gamma}{8\ln(\gamma)} - \Lambda\left[\frac{\gamma^2}{2(1-\gamma)^2(1+\gamma)} - \frac{1+\gamma}{8\ln(\gamma)^2}\right]. \quad (28)$$

Another special case is obtained in the limit $\Lambda \to 0$. In this limit, the buoyancy effect becomes negligible and a pure forced convection regime occurs. By employing Eq. (21) with $\Lambda \to 0$, the integral on the right-hand side of Eq. (23) can be evaluated analytically, so that one obtains

$$u(r) = \frac{C(m,\gamma,0)^m}{2^{1+2m}(1-m)(1-\gamma)^{1+m}} \times \left[r^{1-m}\,{}_2F_1\left(\frac{1-m}{2}, -m; \frac{3-m}{2}; \frac{r^2}{2C(m,\gamma,0)}\right) - \gamma^{1-m}\,{}_2F_1\left(\frac{1-m}{2}, -m; \frac{3-m}{2}; \frac{\gamma^2}{2C(m,\gamma,0)}\right)\right], \quad \text{if } C(m,\gamma,0) > \frac{r^2}{2};$$

$$u(r) = \frac{C(m,\gamma,0)^{(1+m)/2}}{2^{5(1+m)/2}(1-\gamma)^{1+m}\Gamma\left(\frac{3+m}{2}\right)} \times \left[2\Gamma\left(\frac{1-m}{2}\right)\Gamma(1+m) - \Gamma\left(-\frac{1+m}{2}\right)\Gamma(2+m) + 2B_{2C(m,\gamma,0)/r^2}\left(-\frac{1+m}{2}, 1+m\right)\Gamma\left(\frac{3+m}{2}\right) - 2B_{\gamma^2/[2C(m,\gamma,0)]}\left(\frac{1-m}{2}, 1+m\right)\Gamma\left(\frac{3+m}{2}\right)\right], \quad \text{if } \frac{\gamma^2}{2} \le C(m,\gamma,0) \le \frac{r^2}{2};$$

$$u(r) = \frac{1}{2^{2+3m}(1+m)(1-\gamma)^{1+m}} \times \left\{\left[\frac{\gamma^2 - 2C(m,\gamma,0)}{\sqrt{2C(m,\gamma,0)}}\right]^{1+m} {}_2F_1\left(1+m, \frac{1+m}{2}; 2+m; 1-\frac{\gamma^2}{2C(m,\gamma,0)}\right) - \left[\frac{r^2 - 2C(m,\gamma,0)}{\sqrt{2C(m,\gamma,0)}}\right]^{1+m} {}_2F_1\left(1+m, \frac{1+m}{2}; 2+m; 1-\frac{r^2}{2C(m,\gamma,0)}\right)\right], \quad \text{if } C(m,\gamma,0) < \frac{\gamma^2}{2}. \quad (29)$$

In Eq. (29), ${}_2F_1(a, b; w; z)$ denotes the hypergeometric function, $\Gamma(z)$ the Euler gamma function and $B_z(a, b)$ the incomplete Euler beta function. The definitions of these special functions are recalled in the Appendix A, while their most important properties are treated in

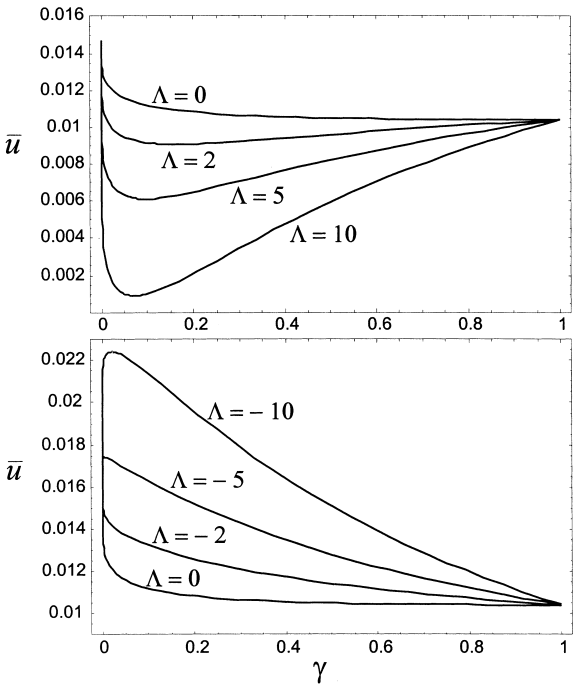

Fig. 2. Plots of $\bar{u}$ vs. γ in the case $m = 1$.

mathematical handbooks such as Gradshteyn and Rhyzik [24]. It must be pointed out that an analysis of the laminar and fully developed velocity profile for isothermal flow of power-law fluids in annular ducts was performed by Fredrickson and Bird [25]. However, although these authors presented their solution in the form of an integral similar to the one reported in Eq. (23), they did not show that an expression in terms of well known special functions could be obtained.

4. A special case: mixed convection of a Newtonian fluid

In this section, the special case of mixed convection for Newtonian fluids, i.e. the case $m = 1$, is analyzed. This analysis is performed by employing Eqs. (25)–(28).

In Figs. 2–4, the behavior of the dimensionless parameters $\bar{u}$, f_1Re and f_2Re as functions of γ is represented, for fixed values of Λ. In particular, in the limit $\gamma \to 0$, the mean dimensionless velocity $\bar{u}$ tends to 1/64, for any value of Λ. As γ increases, Fig. 2 shows that, for positive values of Λ, $\bar{u}$ reaches a minimum and then increases towards the value for $\gamma \to 1$, i.e. 1/96. On the other hand, the plots of $\bar{u}$ vs. γ for $\Lambda < -2$ display the presence of a maximum for very small values of γ. By employing Eq. (27), it is easily shown that, in the limit $\gamma \to 1$, the derivative of $\bar{u}$ with respect to γ is equal to $\Lambda/1440$. Moreover, in the limit $\gamma \to 0$, the derivative of $\bar{u}$ with respect to γ tends to $+\infty$ for $\Lambda < -2$ and to $-\infty$ for $\Lambda > -2$. As a consequence, a value of γ which corresponds to a minimum of the mean dimensionless velocity exists for every positive value of Λ, while a value of γ which corresponds to a maximum of $\bar{u}$ exists for every $\Lambda < -2$.

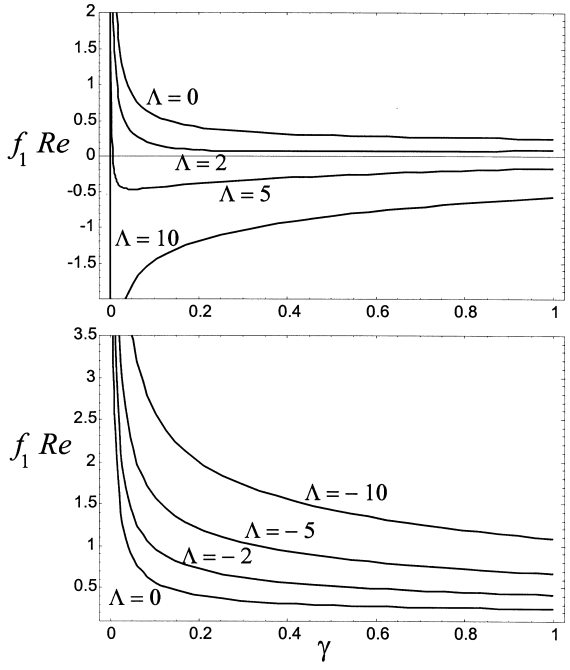

Fig. 3. Plots of f_1Re vs. γ in the case $m = 1$.

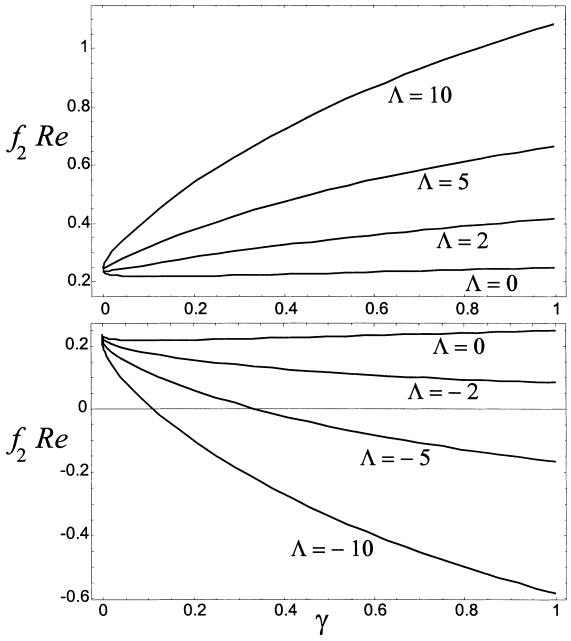

Fig. 4. Plots of f_2Re vs. γ in the case $m = 1$.

Fig. 2 clearly shows that, for a given γ, the dimensionless parameter $\bar{u}$ is a decreasing function of Λ. In other words, for a given axial pressure gradient, buoyancy tends to increase the modulus of the mean fluid velocity, either for upward gradient flow with $T_2 > T_1$ or for downward gradient flow with $T_2 < T_1$. On the contrary, the modulus of the mean velocity is reduced by the buoyancy effect either in the case of downward gradient flow with $T_2 > T_1$ or in the case of upward gradient flow with $T_2 < T_1$.

Figs. 3 and 4 display the behavior of the friction factors as functions of γ both for positive and for negative values of Λ. On account of Eq. (28), it is easily shown that, in the limit $\gamma \to 0$ and for every fixed value of Λ, the parameter f_1Re tends to $+\infty$ and the parameter f_2Re tends to 1/4. For any given $\Lambda \leq 1$, f_1Re is a strictly decreasing function of γ. On the other hand, if $\Lambda > 1$, the parameter f_1Re is a non-monotonic function of γ and displays a minimum for a value of γ which is smaller and smaller as Λ increases. This behavior is quite evident in Fig. 3, although in the case $\Lambda = 10$ the range of the frame is not suitable to represent the minimum reached by f_1Re. By employing Eq. (28), it is

easily shown that the parameter f_2Re, considered as a function of γ for a fixed Λ, is strictly decreasing if $\Lambda \leq -1$, while it displays the occurrence of a minimum for any $\Lambda > -1$. As is shown in Fig. 4, this minimum can correspond to very small values of γ, as in the cases $\Lambda = 2$, 5 and 10. In these cases, if one excludes a very narrow boundary of $\gamma = 0$, f_2Re appears as a monotonic increasing function of γ. Fig. 3 shows that, both for $\Lambda = 5$ and for $\Lambda = 10$, f_1Re becomes negative

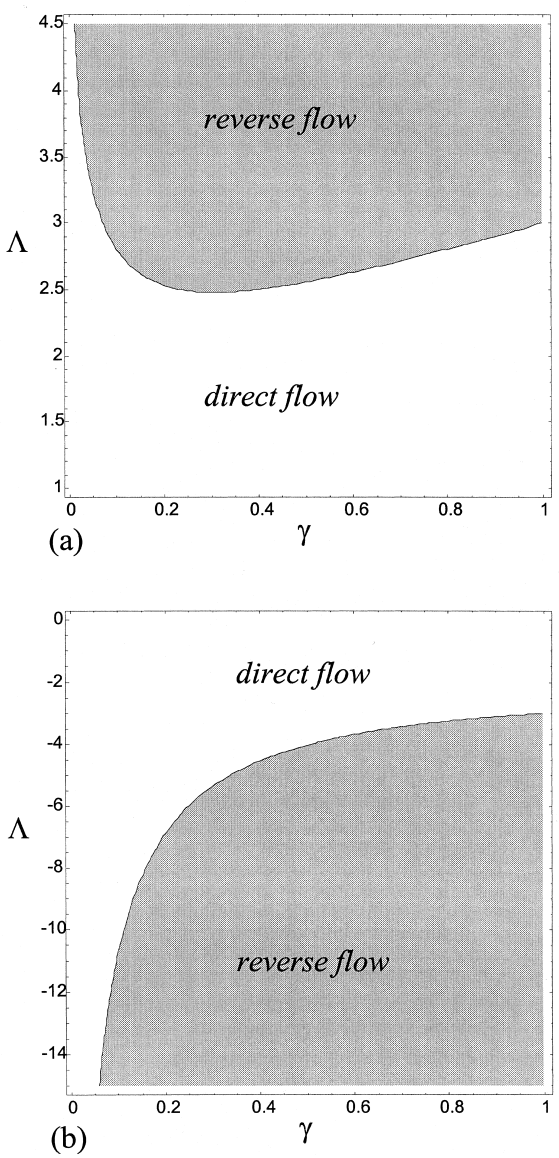

Fig. 5. Drawing of the regions of flow reversal in the plane (γ, Λ) for the case $m = 1$. Frame (a) refers to flow reversal at the inner boundary. Frame (b) refers to flow reversal at the outer boundary.

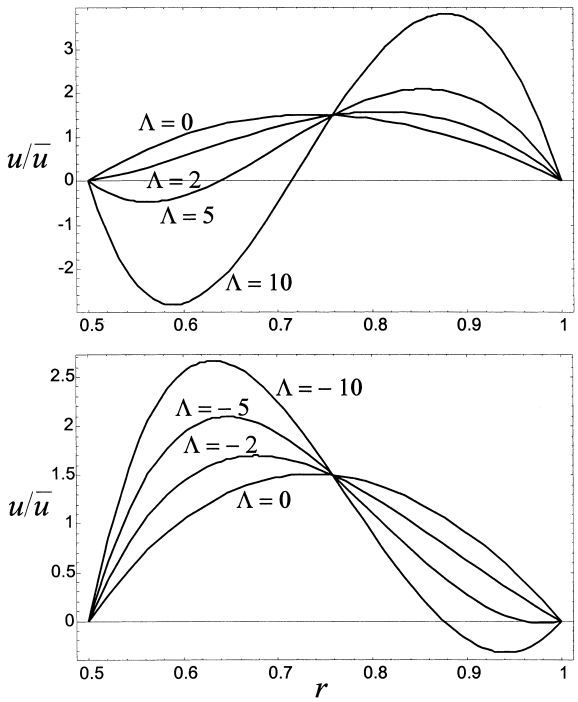

Fig. 6. Plots of $u/\bar{u}$ vs. r for $\gamma = 0.5$ in the case $m = 1$.

even for small values of γ. On the other hand, in Fig. 4, negative values of f_2Re are displayed for $\Lambda = -5$ and for $\Lambda = -10$. As it can be easily verified by employing Eqs. (1) and (17), if f_1Re becomes negative, a flow reversal occurs next to the boundary $R = R_1$. Moreover, if f_2Re becomes negative, a flow reversal occurs next to the boundary $R = R_2$. As is well known, flow reversal occurs when there exists a region next to one of the boundary walls where the quantity $u/\bar{u}$ is negative. Indeed, one can readily show that the onset of flow reversal at a given boundary wall is accompanied by a sign change of both the shear stress and the Fanning friction factor at that boundary wall. An illustration of the regions in the plane (γ, Λ) which correspond to flow reversal either at the inner or at the outer boundary is reported in Fig. 5. The conditions for flow reversal are easily deduced by means of Eq. (28) and are as follows. For positive Λ, flow reversal occurs at the inner boundary whenever

$$\Lambda > \frac{(1-\gamma^2)\left[\gamma^2 - 1 - 2\gamma^2\ln(\gamma)\right]\ln(\gamma)}{(1-\gamma^2)^2 - 4\gamma^2\left[\ln(\gamma)\right]^2}. \tag{30}$$

By employing inequality (30) as well as its graphical representation in Fig. 5(a), it is easily verified that the smallest threshold value of Λ which may yield a flow reversal at the inner surface is $\Lambda = 2.480$ and corresponds to $\gamma = 0.3083$. For negative Λ, the condition

for flow reversal at the outer boundary is

$$|\Lambda| > \frac{(1-\gamma^2)[1-\gamma^2+2\ln(\gamma)]\ln(\gamma)}{(1-\gamma^2)^2-4\gamma^2[\ln(\gamma)]^2}. \quad (31)$$

In this case, on account of inequality (31) and of Fig. 5(b), the smallest threshold value of $|\Lambda|$ is $|\Lambda| = 3$ and corresponds to the limit $\gamma \to 1$, i.e. to the limit of a parallel-plate channel.

In Fig. 6, plots of the dimensionless velocity profiles are reported for $\gamma = 0.5$ and for some positive or negative values of the parameter Λ. This figure shows that, both for $\Lambda = 5$ and for $\Lambda = 10$, the flow reversal phenomena displayed at $r = 0.5$ are more pronounced than those displayed at $r = 1$ for $\Lambda = -5$ and for $\Lambda = -10$. On the other hand, no flow reversal occurs for $\Lambda = 2$ and for $\Lambda = -2$. Moreover, these plots show that, at the position $r = 0.7584$, the ratio $u/\bar{u}$ is unaffected by the value of Λ. Indeed, on account of Eqs. (26) and (27), it can be easily checked that a position r such that the ratio $u/\bar{u}$ is independent of Λ exists for every value of γ. Fig. 6 clearly shows that, if Λ is positive, buoyancy increases the dimensionless velocity $u/\bar{u}$ next to $r = 1$ and decreases $u/\bar{u}$ next to $r = 0.5$. Obviously, the reverse occurs for negative values of Λ. This result is quite reasonable, since a positive value of Λ corresponds either to a downward gradient flow such that $r = 1$ is the hot surface or to an upward gradient flow such that $r = 1$ is the cold surface.

5. A special case: forced convection of a power-law fluid

In this section, the special case of forced convection for power-law fluids, i.e. the case $m \neq 1$ and $\Lambda = 0$, is analyzed. The analysis is performed by employing Eqs. (22), (24) and (29). More precisely, Eq. (22) is solved

Table 1
Values of the parameters $f_1 Re$, $f_2 Re$ and $\bar{u}$, in the case $\Lambda = 0$

m	γ	$f_1 Re$	$f_2 Re$	$\bar{u} \times 10$	m	γ	$f_1 Re$	$f_2 Re$	$\bar{u} \times 10$
0.3	0.01	5.047	0.2020	0.6116	0.5	0.01	4.246	0.2100	0.3855
	0.1	0.7166	0.2033	0.5948		0.1	0.6652	0.2085	0.3664
	0.2	0.4619	0.2076	0.5892		0.2	0.4417	0.2117	0.3605
	0.3	0.3749	0.2125	0.5864		0.3	0.3638	0.2159	0.3576
	0.4	0.3308	0.2177	0.5848		0.4	0.3239	0.2204	0.3559
	0.5	0.3041	0.2230	0.5838		0.5	0.2996	0.2252	0.3549
	0.6	0.2861	0.2283	0.5832		0.6	0.2832	0.2301	0.3543
	0.7	0.2733	0.2337	0.5828		0.7	0.2714	0.2350	0.3539
	0.8	0.2636	0.2391	0.5826		0.8	0.2625	0.2400	0.3537
	0.9	0.2560	0.2446	0.5825		0.9	0.2556	0.2450	0.3536
	1	1/4	1/4	0.5825		1	1/4	1/4	0.3536
0.7	0.01	3.558	0.2169	0.2448	1.5	0.01	1.852	0.2340	4.088×10^{-2}
	0.1	0.6220	0.2128	0.2271		0.1	0.5052	0.2245	3.501×10^{-2}
	0.2	0.4246	0.2151	0.2219		0.2	0.3772	0.2246	3.340×10^{-2}
	0.3	0.3544	0.2187	0.2195		0.3	0.3280	0.2266	3.263×10^{-2}
	0.4	0.3181	0.2228	0.2180		0.4	0.3015	0.2294	3.219×10^{-2}
	0.5	0.2958	0.2271	0.2172		0.5	0.2849	0.2325	3.193×10^{-2}
	0.6	0.2807	0.2316	0.2166		0.6	0.2735	0.2359	3.177×10^{-2}
	0.7	0.2698	0.2362	0.2163		0.7	0.2652	0.2393	3.166×10^{-2}
	0.8	0.2616	0.2408	0.2161		0.8	0.2589	0.2429	3.161×10^{-2}
	0.9	0.2551	0.2454	0.2160		0.9	0.2540	0.2464	3.158×10^{-2}
	1	1/4	1/4	0.2160		1	1/4	1/4	3.157×10^{-2}
2.0	0.01	1.353	0.2390	1.340×10^{-2}	3.5	0.01	0.7610	0.2449	4.761×10^{-4}
	0.1	0.4606	0.2289	1.113×10^{-2}		0.1	0.3854	0.2365	3.799×10^{-4}
	0.2	0.3582	0.2284	1.049×10^{-2}		0.2	0.3240	0.2352	3.493×10^{-4}
	0.3	0.3172	0.2298	1.019×10^{-2}		0.3	0.2972	0.2358	3.345×10^{-4}
	0.4	0.2947	0.2321	1.001×10^{-2}		0.4	0.2819	0.2373	3.261×10^{-4}
	0.5	0.2804	0.2348	9.910×10^{-3}		0.5	0.2719	0.2391	3.210×10^{-4}
	0.6	0.2705	0.2377	9.845×10^{-3}		0.6	0.2648	0.2411	3.178×10^{-4}
	0.7	0.2633	0.2407	9.804×10^{-3}		0.7	0.2596	0.2433	3.158×10^{-4}
	0.8	0.2578	0.2438	9.781×10^{-3}		0.8	0.2557	0.2455	3.146×10^{-4}
	0.9	0.2535	0.2469	9.769×10^{-3}		0.9	0.2525	0.2477	3.140×10^{-4}
	1	1/4	1/4	9.766×10^{-3}		1	1/4	1/4	3.139×10^{-4}

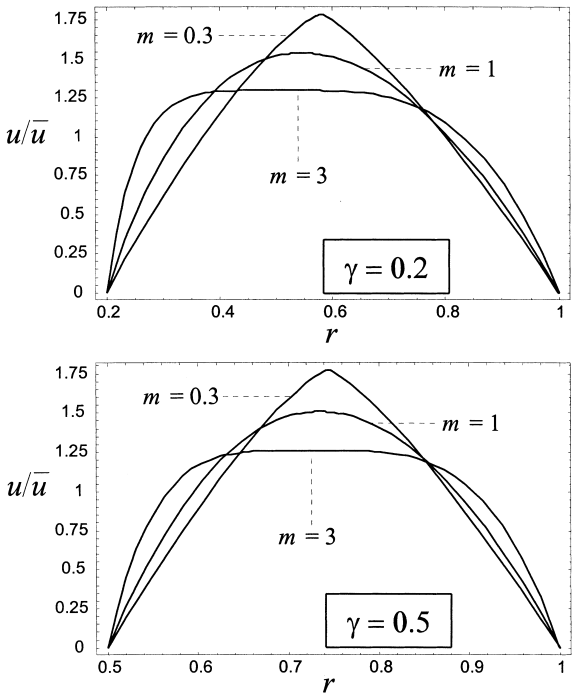

Fig. 7. Plots of $u/\bar{u}$ vs. r for $\gamma = 0.2$ and $\gamma = 0.5$ in the case $\Lambda = 0$.

numerically to determine $C(m, \gamma, 0)$. Then, the friction factors and the dimensionless velocity are evaluated by employing Eqs. (24) and (29).

In Table 1, the values of f_1Re, f_2Re and $\bar{u}$ are reported for some values of m and of γ. In particular, the values of these parameters in the case $\gamma \to 1$ are obtained by employing the results for the parallel-plate channel reported in Ref. [18]. This table reveals that, both for dilatant and for pseudoplastic fluids, the friction factor f_1Re is a decreasing function of γ, while f_2Re is a non-monotonic function of γ which presents a minimum, as in the case $m = 1$ discussed in the preceding section. The behavior of f_1Re is easily verified by considering Fig. 7. In fact, one can check that, as γ decreases, the dimensionless velocity undergoes a steeper radial change in the neighborhood of $r = \gamma$. Another relevant feature of the data reported in Table 1 is the following. For a given γ, the friction factor f_1Re decreases with m, while the other friction factor f_2Re increases with m. Finally, Table 1 reveals that both the change of f_1Re with m at fixed γ and the change of f_1Re with γ at fixed m are more relevant than the corresponding changes of f_2Re, especially for small values of γ.

In Table 2, a comparison between the analytical expression of the velocity profile given by Eq. (29) and the solution found by Fredrickson and Bird [25] is

Table 2
Comparison between the values of $u_{max}/\bar{u}$ obtained by employing Eq. (29) and those reported in Ref. [25]

m	γ	$u_{max}/\bar{u}$ (present paper)	$u_{max}/\bar{u}$ (Ref. [25])	m	γ	$u_{max}/\bar{u}$ (present paper)	$u_{max}/\bar{u}$ (Ref. [25])
0.25	0.01	1.84502	1.869	0.5	0.01	1.75613	1.778
	0.1	1.82375	1.803		0.1	1.70918	1.714
	0.2	1.81391	1.815		0.2	1.69093	1.693
	0.3	1.80846	1.810		0.3	1.68126	1.682
	0.4	1.80513	1.806		0.4	1.67547	1.676
	0.5	1.80302	1.803		0.5	1.67183	1.672
	0.6	1.80167	1.802		0.6	1.66951	1.670
	0.7	1.80082	1.802		0.7	1.66807	1.669
	0.8	1.80032	1.800		0.8	1.66722	1.668
	0.9	1.80007	1.800		0.9	1.66679	1.667
	1	1.80000	–		1	1.66667	–
2.0	0.01	1.53972	1.540	4.0	0.01	1.36558	1.365
	0.1	1.41859	1.419		0.1	1.28018	1.280
	0.2	1.38041	1.380		0.2	1.24569	1.246
	0.3	1.36124	1.361		0.3	1.22744	1.227
	0.4	1.35003	1.350		0.4	1.21653	1.217
	0.5	1.34308	1.344		0.5	1.20969	1.212
	0.6	1.33869	1.340		0.6	1.20534	1.208
	0.7	1.33596	1.337		0.7	1.20263	1.205
	0.8	1.33437	1.336		0.8	1.20103	1.203
	0.9	1.33356	1.334		0.9	1.20023	1.201
	1	1.33333	–		1	1.20000	–

reported. In this table, the values of the ratio $u_{max}/\bar{u}$ for $m = 0.25$, 0.5, 2 and 4, computed by employing Eq. (29), are compared with the corresponding values given in Ref. [25]. The value of u_{max} is easily obtained since, as one can readily infer by employing Eq. (12), when u is maximum σ vanishes. Indeed, if $\Lambda = 0$, Eq. (21) ensures that the radius r which corresponds to $u = u_{max}$ is equal to $\sqrt{2C(m, \gamma, 0)}$. Table 2 reveals that a very good agreement exists with the results obtained in Ref. [25], the relative error being in any case less than 1.3%. The data for $\gamma \to 1$ reported in Table 2 refer to the solution in the case of a parallel-plate channel discussed in Ref. [18].

In Fig. 7, plots of $u/\bar{u}$ vs. r are supplied for $m = 0.3$, 1 and 3, with reference to $\gamma = 0.2$ and 0.5. This figure shows that the plots for $\gamma = 0.5$ have only a slight asymmetry with respect to the mid position $r = (1 + \gamma)/2 = 0.75$, which is less evident in the case of dilatant behavior ($m = 0.3$) than in the case of pseudoplastic behavior ($m = 3$). On the other hand, the plots for $\gamma = 0.2$ are definitely asymmetric with respect to the position $r = (1 + \gamma)/2 = 0.6$. Indeed, for $\gamma = 0.5$, the position of the maximum dimensionless velocity is $r = 0.74436$ if $m = 0.3$, $r = 0.73553$ if $m = 1$, $r = 0.72397$ if $m = 3$. For $\gamma = 0.2$, the maximum dimensionless velocity occurs at $r = 0.57934$ if $m = 0.3$, $r = 0.54611$ if $m = 1$, $r = 0.50299$ if $m = 3$.

Table 3
Values of Λ_r and Λ_r' for different values of m and γ

γ	m	Λ_r	Λ_r'	γ	m	Λ_r	Λ_r'
0.2	0.3	2.0998	4.7004	0.5	0.3	2.0795	3.0446
	0.4	2.1760	5.0401		0.4	2.1630	3.2093
	0.5	2.2465	5.3716		0.5	2.2404	3.3652
	0.6	2.3118	5.6940		0.6	2.3123	3.5130
	0.7	2.3725	6.0064		0.7	2.3794	3.6531
	0.8	2.4293	6.3086		0.8	2.4421	3.7859
	0.9	2.4825	6.6003		0.9	2.5009	3.9119
	1.0	2.5324	6.8817		1.0	2.5562	4.0316
	1.5	2.7431	8.1414		1.5	2.7896	4.5493
	2.0	2.9061	9.1865		2.0	2.9704	4.9613
	2.5	3.0367	10.0604		2.5	3.1152	5.2969
	3.0	3.1440	10.7995		3.0	3.2341	5.5757
	3.5	3.2341	11.4318		3.5	3.3338	5.8112
	4.0	3.3110	11.9786		4.0	3.4188	6.0129
	4.5	3.3775	12.4561		4.5	3.4922	6.1878
	5.0	3.4356	12.8768		5.0	3.5563	6.3410
0.7	0.3	2.1824	2.6643	0.95	0.3	2.3403	2.4089
	0.4	2.2749	2.7958		0.4	2.4455	2.5195
	0.5	2.3608	2.9195		0.5	2.5437	2.6230
	0.6	2.4410	3.0359		0.6	2.6355	2.7199
	0.7	2.5159	3.1456		0.7	2.7216	2.8108
	0.8	2.5861	3.2491		0.8	2.8024	2.8963
	0.9	2.6520	3.3469		0.9	2.8785	2.9769
	1.0	2.7140	3.4395		1.0	2.9503	3.0529
	1.5	2.9768	3.8363		1.5	3.2555	3.3768
	2.0	3.1810	4.1489		2.0	3.4939	3.6302
	2.5	3.3449	4.4020		2.5	3.6856	3.8344
	3.0	3.4796	4.6113		3.0	3.8437	4.0028
	3.5	3.5927	4.7876		3.5	3.9764	4.1443
	4.0	3.6891	4.9382		4.0	4.0897	4.2651
	4.5	3.7724	5.0686		4.5	4.1876	4.3696
	5.0	3.8451	5.1828		5.0	4.2732	4.4609

6. Mixed convection of a power-law fluid

In this section, the general case of mixed convection for power-law fluids is investigated. The analysis is performed by employing Eqs. (21)–(23). Eq. (22) is solved numerically to determine $C(m, \gamma, \Lambda)$. Then, the dimensionless velocity is evaluated by employing Eqs. (21) and (23).

It is easily verified that, for every choice of m and γ, there exist two positive real numbers Λ_r and Λ_r' such that flow reversal at $r = \gamma$ occurs if and only if $\Lambda > \Lambda_r$, while flow reversal at $r = 1$ occurs if and only if $\Lambda < -\Lambda_r'$. In other words, for any given choice of m and γ, the dimensionless shear stress at the inner boundary $\sigma(\gamma)$, i.e. the quantity $f_1 Re$, is positive if $\Lambda < \Lambda_r$ and negative if $\Lambda > \Lambda_r$. Moreover, for any given choice of m and γ, the dimensionless shear stress at the outer boundary $\sigma(1)$, i.e. the quantity $-f_2 Re$, is negative if $\Lambda > -\Lambda_r'$ and positive if $\Lambda < -\Lambda_r'$. The values of Λ_r

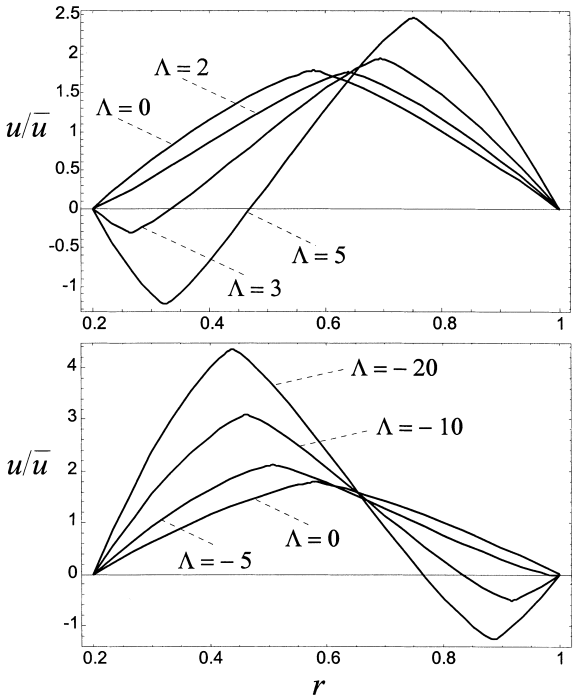

Fig. 8. Plots of $u/\bar{u}$ vs. r for $\gamma = 0.2$ in the case $m = 0.3$.

and Λ_r' are different and, for every m, tend to be equal in the limit $\gamma \to 1$. In fact, in this limit, one yields the parallel-plate channel flow which, as is discussed in Ref. [18], is endowed with a special symmetry linking the upward gradient case ($Re < 0$) and the downward gradient case ($Re > 0$). Values of Λ_r and Λ_r' for given m and γ can be evaluated by employing Eqs. (21), (22) and are reported in Table 3. This table shows that the difference between the values of Λ_r and Λ_r' is specially pronounced for pseudoplastic fluids at low values of γ. In any case, this difference becomes smaller and smaller as γ increases. A comparison between the values of $\Lambda_r = \Lambda_r'$, reported in Ref. [18], for a parallel-plate channel, i.e. for the limit $\gamma \to 1$, and the values of Λ_r and Λ_r' reported in Table 3 for $\gamma = 0.95$ reveals a fair agreement. More precisely, for each m, the value of Λ_r for $\gamma = 0.95$ is slightly lower than that for $\gamma \to 1$, while the value of Λ_r' for $\gamma = 0.95$ is slightly higher than that for $\gamma \to 1$. For a given m, the change of Λ_r' with γ is much more sharp than that of Λ_r. It is easily verified that, for a fixed m, while Λ_r' is a monotonic decreasing function of γ, Λ_r is a non-monotonic function of γ. In fact, for a given value of m, the qualitative behavior of Λ_r as a function of γ is the same as that outlined in the preceding sections with reference to Newtonian fluids and illustrated in Fig. 5(a). More precisely, for a fixed value of m, it can be shown that Λ_r decreases for small γ, reaches a minimum and then increases.

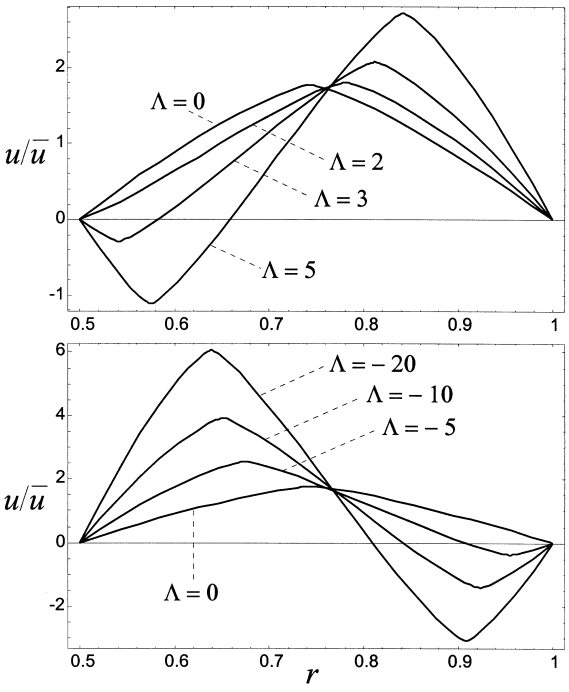

Fig. 10. Plots of $u/\bar{u}$ vs. r for $\gamma = 0.5$ in the case $m = 0.3$.

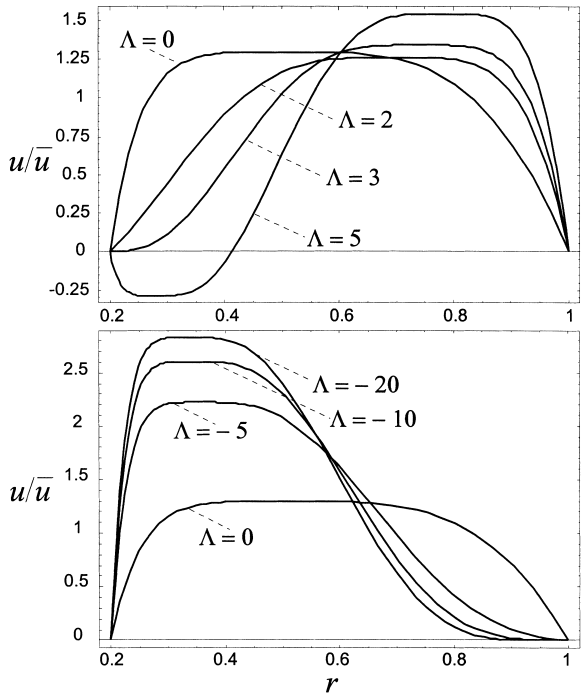

Fig. 9. Plots of $u/\bar{u}$ vs. r for $\gamma = 0.2$ in the case $m = 3$.

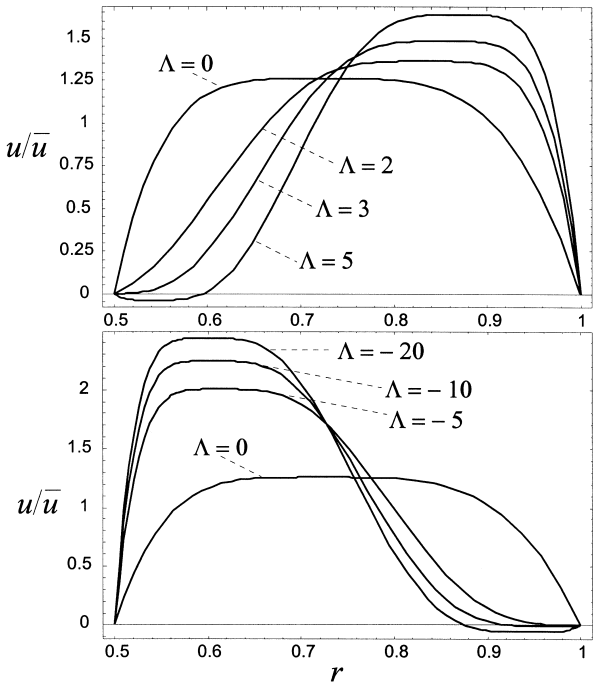

Fig. 11. Plots of $u/\bar{u}$ vs. r for $\gamma = 0.5$ in the case $m = 3$.

An analysis of Table 3 allows one to conclude that the onset of a flow reversal at $r = 1$ requires an higher wall temperature difference than the onset of a flow reversal at $r = \gamma$. Moreover, the smaller is the value of γ, the higher is the value of $|\Lambda|$ which yields a flow reversal at $r = 1$. Finally, it should be pointed out that, for every γ, both Λ_r and Λ_r' are increasing functions of m. As a consequence, dilatant fluids need smaller values of $|\Lambda|$ than pseudoplastic fluids in order to display flow reversal. This feature was already pointed out with reference to parallel-plate channels [18].

Figs. 8–11 display the dimensionless velocity $u(r)/\bar{u}$ for different values of Λ, with reference either to a dilatant fluid with $m = 0.3$ or to a pseudoplastic fluid with $m = 3$. In these figures, the values $\gamma = 0.2$ (Figs. 8 and 9) and $\gamma = 0.5$ (Figs. 10 and 11) are considered. Fig. 8, which refers to $\gamma = 0.2$ and $m = 0.3$, shows that flow reversal occurs for $\Lambda = 3$ and 5 next to $r = 0.2$, while flow reversal occurs in the neighborhood of $r = 1$ for $\Lambda = -10$, for $\Lambda = -20$ and, although hardly perceptible, for $\Lambda = -5$. These circumstances are compatible with the threshold values Λ_r and Λ_r' reported in Table 3, namely $\Lambda_r = 2.0998$ and $\Lambda_r' = 4.7004$. In Fig. 9, the case $\gamma = 0.2$ and $m = 3$ is considered. This figure reveals a flow reversal next to the inner boundary, for $\Lambda = 5$. On the other hand, the scale of the plots is not suitable to perceive the flow reversal occurring next to $r = 1$, for $\Lambda = -20$. Indeed, Table 3 implies that, in this case, the threshold values for the onset of flow reversal are $\Lambda_r = 3.1440$ and $\Lambda_r' = 10.7995$. In Fig. 10, as in Fig. 8, flow reversals exist for $\Lambda = 3$ and 5, as well as for $\Lambda = -5$, -10 and -20. However, one of the most visible differences between Figs. 8 and 10 is that Fig. 10, which refers to $\gamma = 0.5$ and $m = 0.3$, displays a completely evident flow reversal at $\Lambda = -5$. This conclusion agrees with the statement that an increase of γ implies an enhancement of flow reversal at $r = 1$. In fact, on account of Table 3, if $m = 0.3$ and γ varies from 0.2 to 0.5, Λ_r' undergoes a change from 4.7004 to 3.0446. On the other hand, Table 3 shows that, for $m = 0.3$, Λ_r undergoes a slight change in the range $0.2 < \gamma < 0.5$. In other words, as it can be also inferred by comparing Figs. 8 and 10, the phenomenon of flow reversal at the inner boundary is not much different in the cases $\gamma = 0.2$ and 0.5. The comparison between Fig. 9, which refers to $\gamma = 0.2$ and $m = 3$, and Fig. 11, which refers to $\gamma = 0.5$ and $m = 3$, leads to the following conclusions. When $\gamma = 0.5$, the flow reversal at $r = 1$ for $\Lambda = -20$ is slightly enhanced; a flow reversal for $\Lambda = -10$ appears which does not occur when $\gamma = 0.2$; flow reversal at the inner boundary for $\Lambda = 5$ is much less evident. Hence, the increase of γ from 0.2 to 0.5 implies an enhanced flow reversal at the outer boundary and, in the case $m = 3$, a definitely inhibited flow reversal at the inner boundary.

7. Conclusions

Mixed convection of a power-law fluid in a vertical annular duct has been investigated in a regime of laminar and fully developed flow. Uniform and unequal temperatures have been prescribed on the inner and outer boundary walls. The local energy and momentum balance equations as well as the stress–strain constitutive relation have been written in a dimensionless form.

It has been pointed out that the dimensionless solution is uniquely determined by the inverse of the power-law index m, by the ratio γ between the duct inner and outer radii and by the ratio Λ between the Grashof number Gr and the Reynolds number Re. The dimensionless temperature has been shown to be the same as in the case of pure conduction and to be independent of m and of Λ. On the other hand, both the dimensionless shear stress and the dimensionless velocity depend appreciably on m, γ and Λ.

Analytical expressions which allow the determination of the dimensionless velocity and of the friction factors have been obtained. The special cases of mixed convection for Newtonian fluids and of forced convection for power-law fluids have been analyzed. In the first special case, it has been shown that the conditions for the onset of flow reversal imply the existence of threshold values for $|\Lambda|$, which depend on γ. When these threshold values are exceeded, flow reversal occurs either next to the inner boundary wall or next to the outer boundary wall. In the second special case, an analytical expression of the dimensionless velocity distribution has been obtained and a comparison with the results reported by Fredrickson and Bird [25] has been performed, revealing a fair agreement.

In the general case of mixed convection for power-law fluids, the flow reversal conditions have been investigated. As for Newtonian fluids, flow reversal occurs when threshold values of $|\Lambda|$ are exceeded. These threshold values depend both on γ and on m and, for a fixed value of γ, are increasing functions of m. As a consequence, dilatant fluids need smaller values of $|\Lambda|$ than pseudoplastic fluids in order to display flow reversal. For a fixed m, the threshold value of $|\Lambda|$ for the onset of flow reversal at the outer boundary is a monotonic increasing function of γ. On the other hand, the threshold value of $|\Lambda|$ for the onset of flow reversal at the inner boundary depends non-monotonically on γ. More precisely, for every m, there exists a value of γ such that this threshold value is minimum.

Appendix A

The hypergeometric function is defined as

$$ {}_2F_1(a, b; w; z) = \frac{\Gamma(w)}{\Gamma(a)\Gamma(b)} \sum_{j=0}^{\infty} \frac{\Gamma(a+j)\Gamma(b+j)}{j!\Gamma(w+j)} z^j. $$

The Euler gamma function is defined as

$$ \Gamma(z) = \int_0^{\infty} t^{z-1} \mathrm{e}^{-t}\, \mathrm{d}t. $$

The incomplete Euler beta function is defined as

$$ B_z(a, b) = \int_0^{z} t^{a-1}(1-t)^{b-1}\, \mathrm{d}t. $$

References

[1] A.B. Metzner, Heat transfer in non-Newtonian fluids, Advances in Heat Transfer 2 (1965) 357–397.

[2] Y.I. Cho, J.P. Hartnett, Non-Newtonian fluids in circular pipe flow, Advances in Heat Transfer 15 (1982) 59–141.

[3] A.V. Shenoy, R.A. Mashelkar, Thermal convection in non-Newtonian fluids, Advances in Heat Transfer 15 (1982) 143–225.

[4] T.F. Irvine, J. Karni, Non-Newtonian fluid flow and heat transfer, in: S. Kakaç, R.K. Shah, W. Aung (Eds.), Handbook of Single-Phase Convective Heat Transfer, Wiley, New York, 1987 (Chapter 20).

[5] J.P. Hartnett, M. Kostic, Heat transfer to Newtonian and non-Newtonian fluids in rectangular ducts, Advances in Heat Transfer 19 (1989) 247–356.

[6] S.X. Gao, J.P. Hartnett, Non-Newtonian fluid laminar flow and forced convection heat transfer in rectangular ducts, International Communications in Heat and Mass Transfer 19 (1992) 673–686.

[7] M. Capobianchi, T.F. Irvine Jr, Predictions of pressure drop and heat transfer in concentric annular ducts with modified power law fluids, Wärme- und Stoffübertragung 27 (1992) 209–215.

[8] J. Prusa, R.M. Manglik, Asymptotic and numerical solutions for thermally developing flows of Newtonian and non-Newtonian fluids in circular tubes with uniform wall temperature, Numerical Heat Transfer A26 (1994) 199–217.

[9] S.G.H. Etemad, A.S. Mujumdar, Effects of variable viscosity and viscous dissipation on laminar convection heat transfer of a power law fluid in the entrance region of a semi-circular duct, International Journal of Heat and Mass Transfer 38 (1995) 2225–2238.

[10] A. Barletta, Fully developed laminar forced convection in circular ducts for power-law fluids with viscous dissipation, International Journal of Heat and Mass Transfer 40 (1997) 15–26.

[11] T. Min, J.Y. Yoo, H. Choi, Laminar convective heat transfer of a Bingham plastic in a circular pipe—I. Analytical approach — thermally fully developed flow and thermally developing flow (the Graetz problem extended), International Journal of Heat and Mass Transfer 40 (1997) 3025–3037.

[12] T. Min, H.G. Choi, J.Y. Yoo, H. Choi, Laminar convective heat transfer of a Bingham plastic in a circular pipe—II. Numerical approach — hydrodynamically developing flow and simultaneously developing flow, International Journal of Heat and Mass Transfer 40 (1997) 3689–3701.

[13] S. Khellaf, G. Lauriat, A new analytical solution for heat transfer in the entrance region of ducts: hydrodynamically developed flows of power-law fluids with constant wall temperature, International Journal of Heat and Mass Transfer 40 (1997) 3443–3447.

[14] A. Lawal, D.M. Kalyon, Nonisothermal extrusion flow of viscoplastic fluids with wall slip, International Journal of Heat and Mass Transfer 40 (1997) 3883–3897.

[15] S. Olek, Heat transfer in duct flow of non-Newtonian fluids with axial conduction, International Communications in Heat and Mass Transfer 25 (1998) 929–938.

[16] A.T. Jones, D.B. Ingham, Combined convection flow and heat transfer to a power law fluid in a vertical duct including reverse flow situations, Numerical Heat Transfer A25 (1994) 57–73.

[17] D.B. Ingham, A.T. Jones, Combined convection flow of a power-law fluid in a vertical duct with linearly varying wall temperatures, Acta Mechanica 110 (1995) 19–32.

[18] A. Barletta, On fully-developed mixed convection and flow reversal of a power-law fluid in a vertical channel, International Communications in Heat and Mass Transfer 26 (1999) 1127–1137.

[19] K. Sherwin, Laminar convection in uniformly heated vertical concentric annuli, British Chemical Engineering 13 (1968) 1580–1585.

[20] M.S. Rokerya, M. Iqbal, Effects of viscous dissipation on combined free and forced convection through vertical concentric annuli 14 (1971) 491–495.

[21] D. Maitra, K. Sabba Raju, Combined free and forced convection laminar heat transfer in a vertical annulus, ASME Journal of Heat Transfer 97 (1975) 135–137.

[22] H.-S. Kou, D.-K. Huang, Fully developed laminar mixed convection through a vertical annular duct filled with porous media, International Communications in Heat and Mass Transfer 24 (1997) 99–110.

[23] A. Barletta, E. Zanchini, On the choice of the reference temperature for fully-developed mixed convection in a vertical channel, International Journal of Heat and Mass Transfer 42 (1999) 3169–3181.

[24] I.S. Gradshteyn, I.M. Ryzhik, Table of Integrals, Series and Products, Academic Press, Orlando, FL, 1980.

[25] A.G. Fredrickson, R.B. Bird, Non-Newtonian flow in annuli, Industrial and Engineering Chemistry 50 (1958) 347–352; Errata Corrige in Industrial and Engineering Chemistry — Fundamentals 3 (1964) 383.